SUPPLEMENT FIGURES AND TABLES

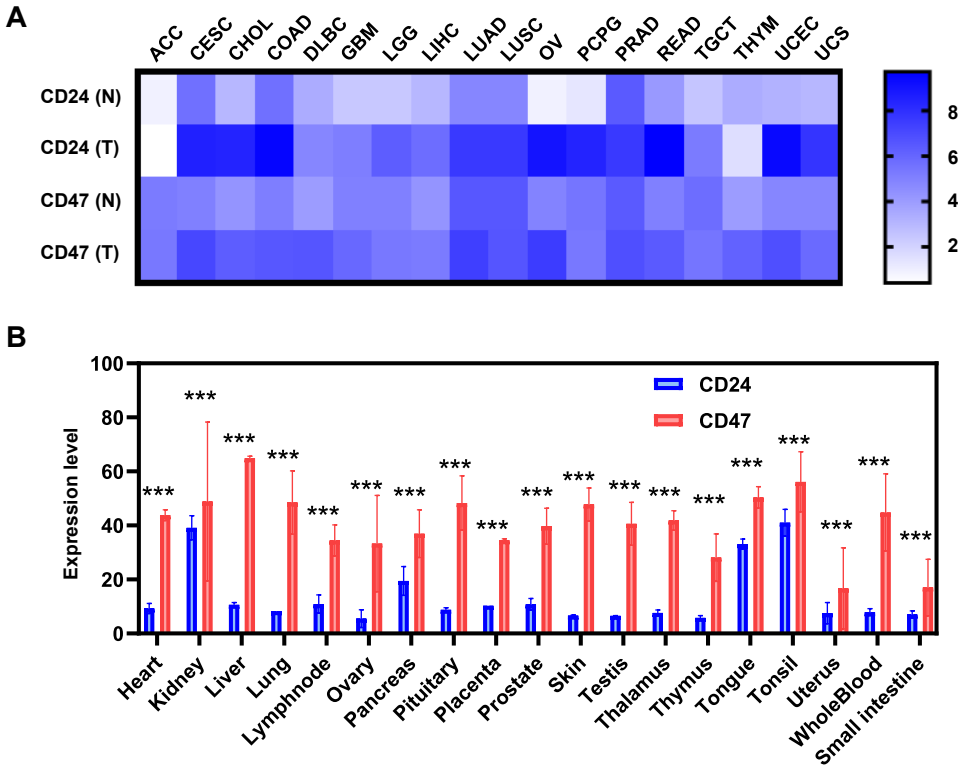

Fig. S1 Expression of CD24 and CD47 in multiple human cancers or normal tissues.

(A) Heatmap of expression of CD24 and CD47 across multiple human cancers compared to corresponding normal tissues obtained from UALCAN database. (B) Analysis of the expression of CD24 and CD47 in different organs by BioGPS. Data are presented as means ± SEM, and statistical significance was determined by unpaired Student's *t*-test. ****P* < *0.001*.

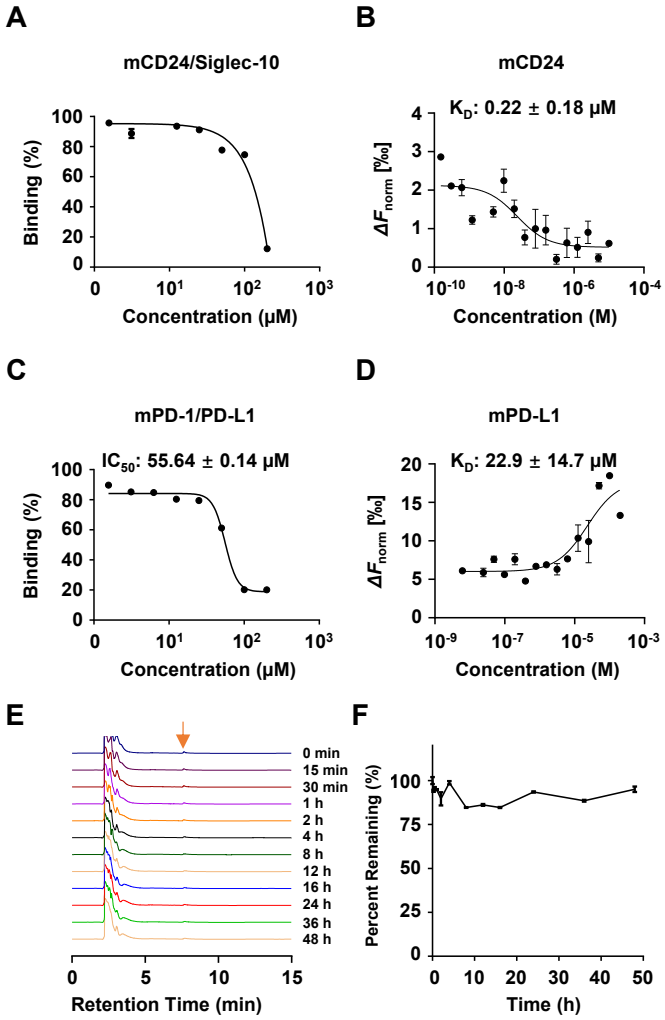

Fig. S2 *In vitro* blocking activity and serum stability of CSBP.

(A) *In vitro* blocking activity of CSBP on the mouse CD24/hSiglec-10 interaction as measured by flow cytometry. (B) *In vitro* binding affinity of CSBP on mouse CD24 as measured by MST. (C) *In vitro* blocking activity of CSBP on the mouse PD-1/PD-L1 interaction as measured by flow cytometry. (D) Binding affinity of CSBP on mouse PD-L1 as measured by MST. (E) Representative HPLC analysis of CSBP hydrolysis in 10% mouse serum. (F) The residual peptide time-dependent curve. Data are presented as means ± SEM.

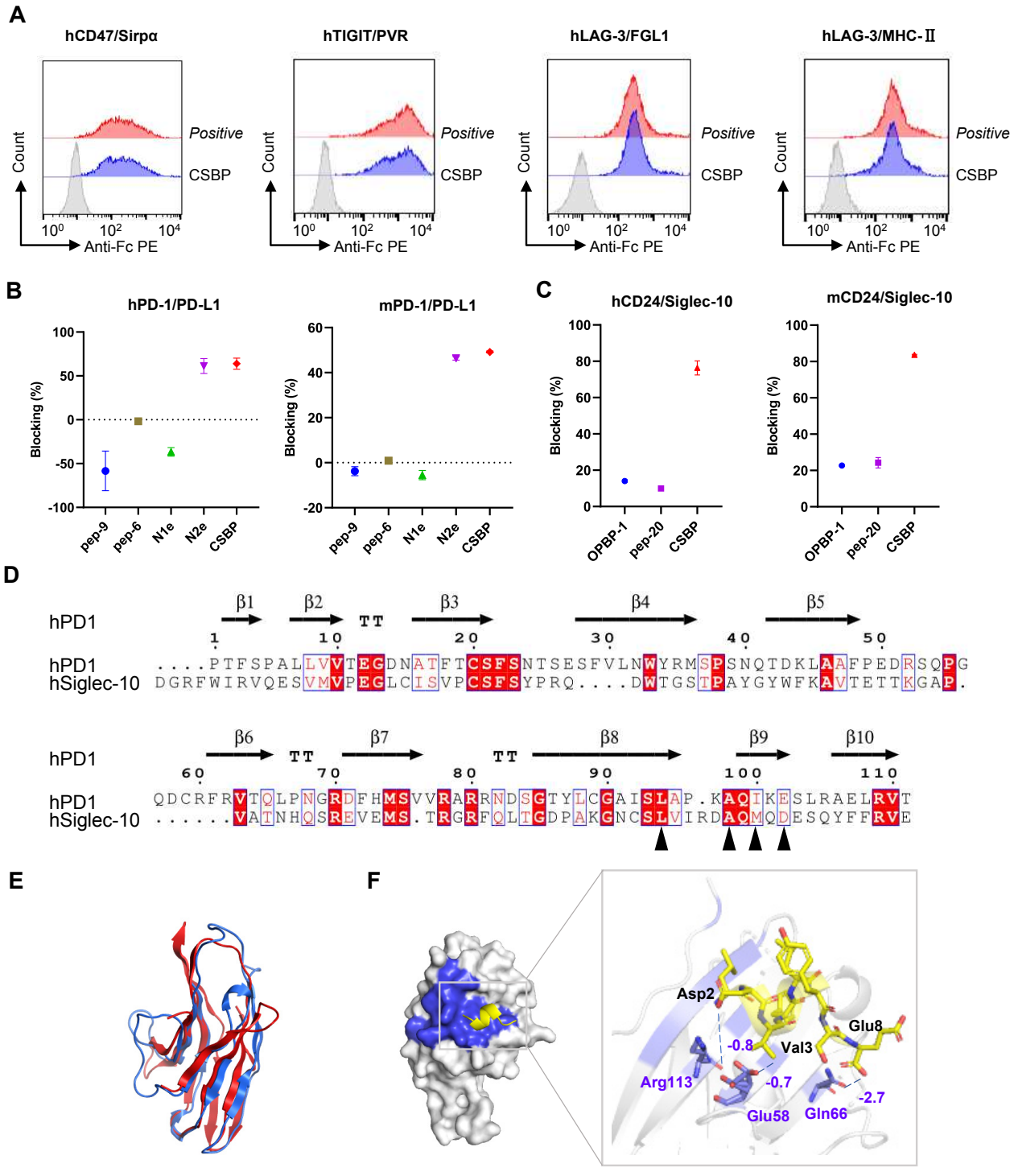

Fig. S3 The specificity of CSBP to block CD24/Siglec-10 and PD-1/PD-L1 interactions.

(A) *In vitro* blocking activity of CSBP was measured by flow cytometry on the human CD47/Sirpα, TIGIT/PVR, LAG-3/FGL1 and LAG-3/MHC-Ⅱ. (B) *In vitro* blocking activity of pep-9, pep-6, N1e, N2e and CSBP on the PD-1/PD-L1 interaction was measured by flow cytometry. (C) *In vitro* blocking activity of OPBP-1, pep-20 and CSBP on the CD24/Siglec-10 was measured by flow cytometry. (D) Alignment of Siglec-10 and PD-1 IgV domain sequences. Binding sites of PD-L1 to PD-1 were indicated by bold triangular. (E) Structural alignment of the predicted 3D structures of Siglec-10 (blue) and PD-1 (red). (F) The binding model of CSBP (yellow) and PD-L1 (gray) with binding area shown in blue. The key residues and binding energy (blue) of CSBP/PD-L1. Data are presented as means ± SEM.

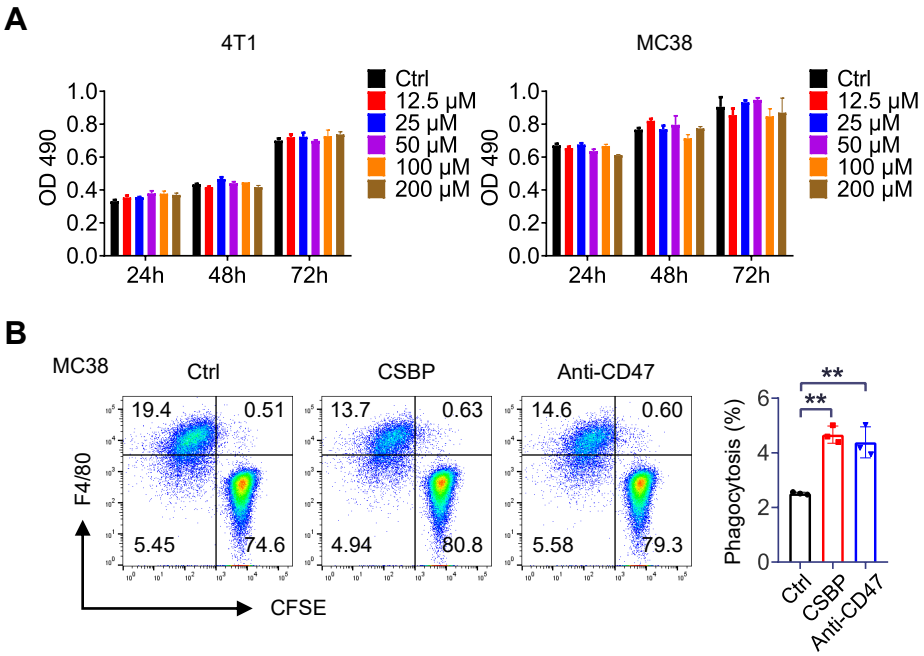

Fig. S4 CSBP promotes phagocytosis of MC38 cells by macrophage.

(A) MTT assay demonstrates that CSBP has no effect on the viability of 4T1 and MC38 cells. (B) MC38 cells were stained with CFSE, incubated with bone marrow-derived macrophages for 2 h, stained with F4/80 antibody, subjected to flow cytometry, and the percentage of $CFSE^+$ $F4/80^+$ phagocytosed cancer cells was determined. Data are presented as means ± SEM, and statistical significance was determined by two-way ANOVA with multiple comparisons. $^{**}P < 0.01$.

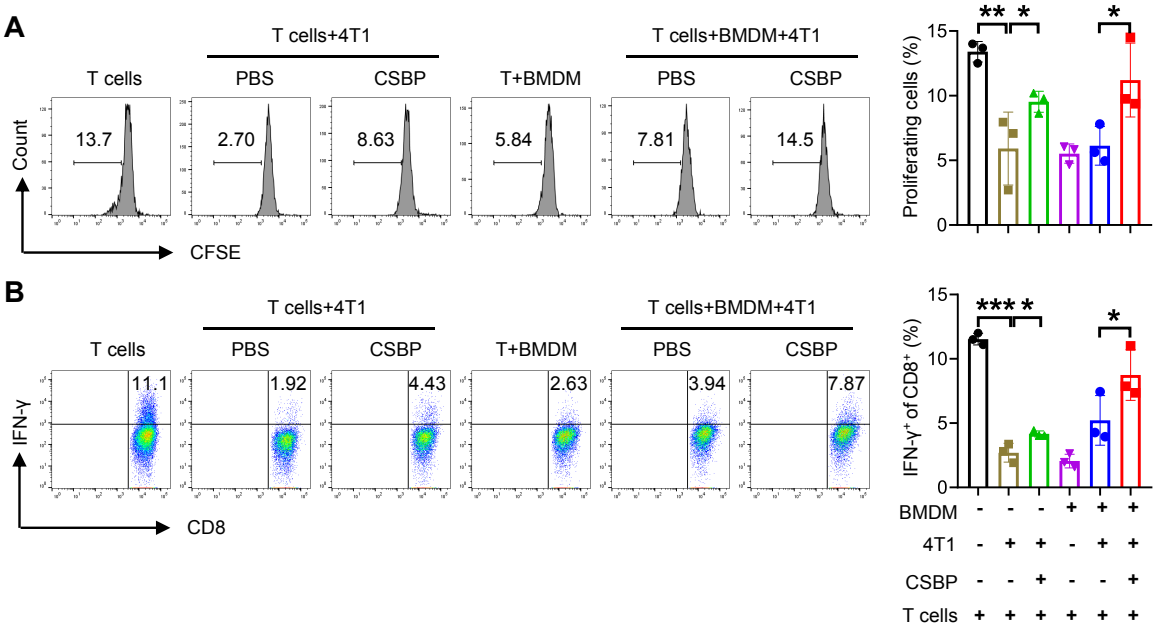

Fig. S5 Macrophages prime CD8⁺ T cells to proliferate after phagocytosis of 4T1 cancer cells mediated by CSBP.

(A, B) Bone marrow-derived macrophages (BMDM) were cocultured with 4T1 cells at a ratio of 1:4 in the presence of CSBP. The next day, CD8⁺ T cells from 4T1 tumor-bearing mice were labeled with CFSE (0.5 μM). Analysis was performed on day 3, and the proliferation of CD8⁺ T cells and proportion of IFN-γ⁺ CD8⁺ T cells were determined. Data are representative of at least three independent experiments. Data are presented as means ± SEM, and statistical significance was determined by unpaired Student's *t*-test. **P < 0.05, **P < 0.01, ***P < 0.001.*

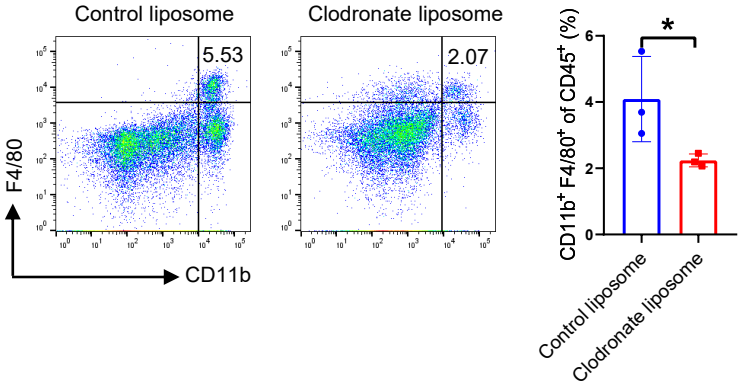

Fig. S6 Depletion of macrophages by clodronate liposome *in vivo*. For macrophage depletion, C57BL/6 mice were injected *i.p.* with 150 μL of clodronate liposomes or control liposomes, then peripheral blood was isolated from the mice 3 days later. The percentage of $CD45^+$ $CD11b^+$ $F4/80^+$ macrophages was evaluated by flow cytometry. Data are presented as means ± SEM, and statistical significance was determined by unpaired Student's *t*-test. $*P < 0.05$.

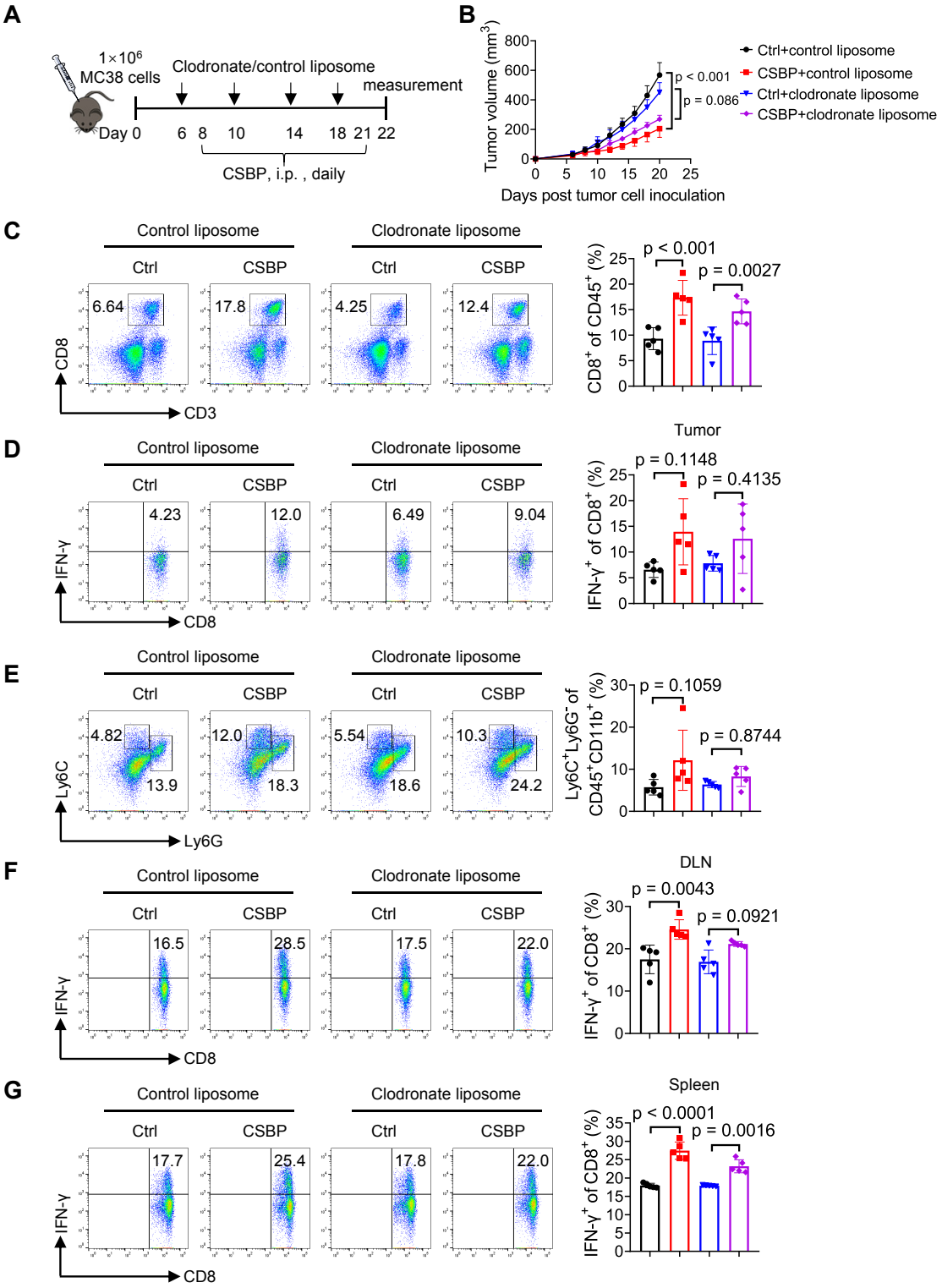
A
1×10^6
MC38 cells
Clodronate/control liposome
measurement
Day 0
6 8 10 14 18 21 22
CSBP, i.p. , daily
B
Tumor volume (mm^3)
Days post tumor cell inoculation
Ctrl+control liposome
CSBP+control liposome
Ctrl+clodronate liposome
CSBP+clodronate liposome
p < 0.001
p = 0.086
C
Control liposome
Clodronate liposome
Ctrl
CSBP
6.64
17.8
4.25
12.4
CD8
CD3
CD8+ of CD45+ (%)
p < 0.001
p = 0.0027
D
4.23
12.0
6.49
9.04
IFN-γ
CD8
Tumor
IFN-γ+ of CD8+ (%)
p = 0.1148
p = 0.4135
E
4.82
13.9
12.0
18.3
5.54
18.6
10.3
24.2
Ly6C
Ly6G
Ly6C+Ly6G- of CD45+CD11b+ (%)
p = 0.1059
p = 0.8744
F
16.5
28.5
17.5
22.0
DLN
IFN-γ+ of CD8+ (%)
p = 0.0043
p = 0.0921
G
17.7
25.4
17.8
22.0
Spleen
p < 0.0001
p = 0.0016

Fig. S7 Depletion of macrophages impairs the antitumor efficacy of CSBP in MC38 tumor model. (A) Schematic of the dosing schedule time points for treatment groups. (B) The tumor growth curves of MC38-bearing mice receiving the treatment of CSBP. Data are presented as the means ± SEM (*n* = 5 per group). (C) The percentage of tumor-infiltrating $CD8^+$ T cells in total $CD45^+$ cells was determined by flow cytometry (*n* = 5). (D) The frequency of IFN-γ-expressing $CD8^+$ T cells was detected by flow cytometry (*n* = 5). (E) Percentages of MDSC within the TME in each group (*n* = 5). G-MDSC, $CD45^+$ $CD11b^+$ $Ly6G^+$ $Ly6C^-$; M-MDSC, $CD45^+$ $CD11b^+$ $Ly6G^-$ $Ly6C^+$. (F, G) Cells from mice draining lymph nodes (F) or spleens (G) were obtained and stimulated with 20 ng/mL of PMA and 1 μM ionomycin containing protein transport inhibitor cocktail for 4 h. Frequencies of IFN-γ-expressing $CD8^+$ T cells were detected by flow cytometry (*n* = 5). Data are presented as means ± SEM, and statistical significance was determined by two-way ANOVA with multiple comparisons.

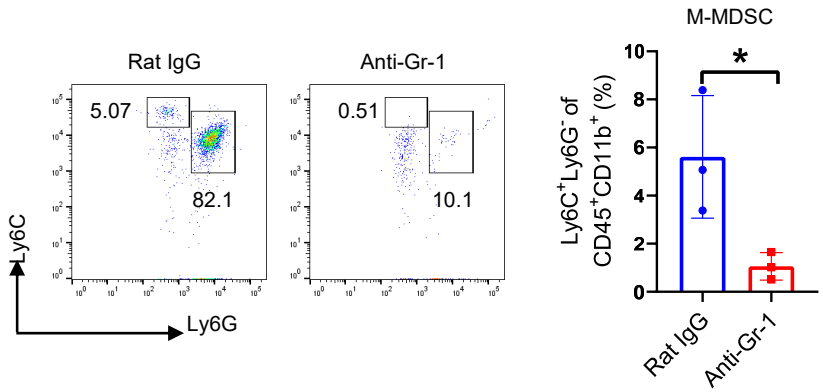

Fig. S8 Depletion of M-MDSCs by anti-Gr-1 *in vivo*. For MDSC depletion, C57BL/6 mice were injected *i.p.* with 100 μg of anti-Gr-1 or Rat IgG, then peripheral blood was isolated from the mice 3 days later. The percentage of M-MDSC ($CD45^+$ $CD11b^+$ $Ly6G^-$ $Ly6C^+$) was evaluated by flow cytometry. Data are presented as means ± SEM, and statistical significance was determined by unpaired Student's *t*-test. $*P < 0.05$.

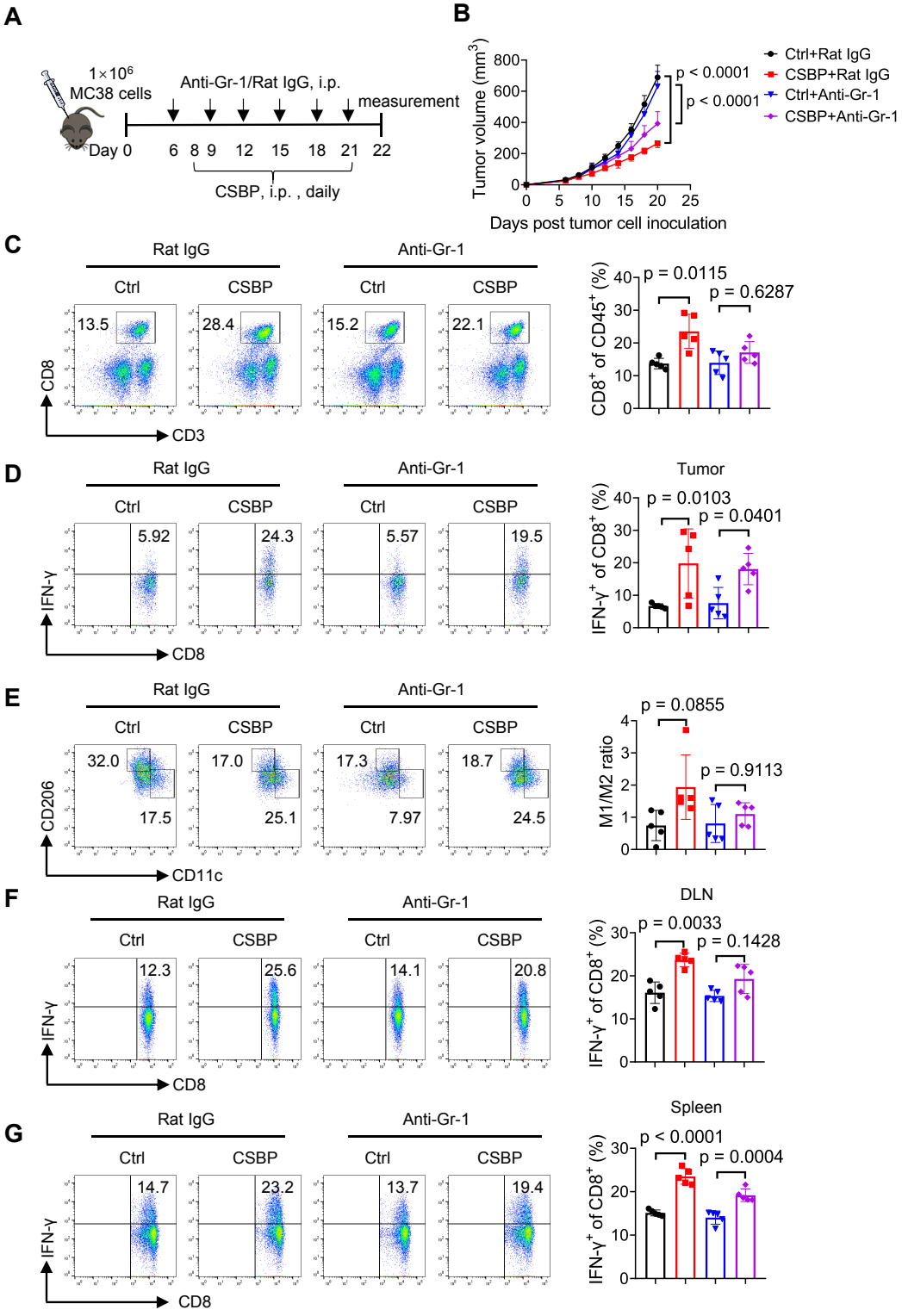
A
1×10^6 MC38 cells
Anti-Gr-1/Rat IgG, i.p.
measurement
Day 0 6 8 9 12 15 18 21 22
CSBP, i.p. , daily
B
Tumor volume (mm^3)
Days post tumor cell inoculation
p < 0.0001
p < 0.0001
Ctrl+Rat IgG
CSBP+Rat IgG
Ctrl+Anti-Gr-1
CSBP+Anti-Gr-1
C
Rat IgG
Anti-Gr-1
Ctrl
CSBP
13.5
28.4
15.2
22.1
CD8
CD3
CD8+ of CD45+ (%)
p = 0.0115
p = 0.6287
D
IFN-γ
CD8
5.92
24.3
5.57
19.5
Tumor
IFN-γ+ of CD8+ (%)
p = 0.0103
p = 0.0401
E
CD206
CD11c
32.0
17.5
17.0
25.1
17.3
7.97
18.7
24.5
M1/M2 ratio
p = 0.0855
p = 0.9113
F
12.3
25.6
14.1
20.8
DLN
p = 0.0033
p = 0.1428
G
14.7
23.2
13.7
19.4
Spleen
p < 0.0001
p = 0.0004

Fig. S9 The antitumor effect of CSBP is partially dependent on M-MDSCs.

(A) Schematic of the dosing schedule time points for treatment groups. (B) The tumor growth curves of MC38-bearing mice receiving the treatment of CSBP. Data are presented as the mean ± SEM (*n* = 5 per group). (C) The percentage of tumor-infiltrating $CD8^+$ T cells in total $CD45^+$ cells was determined by flow cytometry (*n* = 5). (D) The frequency of IFN-γ-expressing $CD8^+$ T cells was detected by flow cytometry (*n* = 5). (E) Radio of M1/M2 within the TME in each group (*n* = 5). M1, $CD45^+$ $CD11b^+$ $F4/80^+$ $CD11c^+$ $CD206^-$; M2, $CD45^+$ $CD11b^+$ $F4/80^+$ $CD206^+$ $CD11c^-$. (F, G) Cells from mice draining lymph nodes (F) or spleens (G) were obtained and stimulated with 20 ng/mL of PMA and 1 μM ionomycin containing protein transport inhibitor cocktail for 4 h. Frequencies of IFN-γ-expressing $CD8^+$ T cells were detected by flow cytometry (*n* = 5). Data are presented as means ± SEM, and statistical significance was determined by two-way ANOVA with multiple comparisons.

Table S1. Enriched CD24-binding phage clones

Name	Sequence	Frequency (n/56)	Blocking rate (%)
1	WSLGYTG	16	2.69 ± 3.80
2	LVTVHYS	16	9.79 ± 0.47
3	GSAPLEG	1	10.27 ± 5.29
4	HLTSERL	1	5.53 ± 9.58
5	GMNRLDI	1	18.43 ± 0.52
6	FTSTHHA	1	39.03 ± 11.98
7	VTKLVTV	1	14.46 ± 6.10
8	CTLMFGL	1	1.44 ± 2.49
9	SYLFVDL	1	55.70 ± 1.24

Table S2. The blocking activity of alanine scan peptides of BP to CD24/Siglec-10 interaction

Name	Sequence	Blocking rate (%)
BP	SYLFVDL	69.41 ± 7.26
1A	AYLFVDL	20.11 ± 3.92
2A	SALFVDL	26.43 ± 2.07
3A	SYAFVDL	-17.79 ± 4.09
4A	SYLAVDL	-11.27 ± 1.30
5A	SYLFADL	-3.59 ± 0.60
6A	SYLFVAL	42.21 ± 8.27
7A	SYLFVDA	40.14 ± 5.30